JCI insight

Fatty acid receptor modulator PBI-4050 inhibits kidney fibrosis and improves glycemic control

Yan Li, … , Ming-Zhi Zhang, Raymond C. Harris

JCI Insight. 2018;3(10):e120365. https://doi.org/10.1172/jci.insight.120365.

Research Article Nephrology

Extensive kidney fibrosis occurs in several types of chronic kidney diseases. PBI-4050, a potentially novel first-in-class orally active low–molecular weight compound, has antifibrotic and antiinflammatory properties. We examined whether PBI-4050 affected the progression of diabetic nephropathy (DN) in a mouse model of accelerated type 2 diabetes and in a model of selective tubulointerstitial fibrosis. eNOS$^{-/-}$ *db/db* mice were treated with PBI-4050 from 8–20 weeks of age (early treatment) or from 16–24 weeks of age (late treatment). PBI-4050 treatment ameliorated the fasting hyperglycemia and abnormal glucose tolerance tests seen in vehicle-treated mice. In addition, PBI-4050 preserved (early treatment) or restored (late treatment) blood insulin levels and increased autophagy in islets. PBI-4050 treatment led to significant improvements in lifespan in the diabetic mice. Both early and late PBI-4050 treatment protected against progression of DN, as indicated by reduced histological glomerular injury and albuminuria, slow decline of glomerular filtration rate, and loss of podocytes. PBI-4050 inhibited kidney macrophage infiltration, oxidative stress, and TGF-β–mediated fibrotic signaling pathways, and it also protected against the development of tubulointerstitial fibrosis. To confirm a direct antiinflammatory/antifibrotic effect in the kidney, further studies with a nondiabetic model of EGFR-mediated proximal tubule activation confirmed that PBI-4050 dramatically decreased the development of the associated tubulointerstitial injury and macrophage infiltration. These studies suggest that PBI-4050 attenuates development of DN in type 2 […]

JCI insight

RESEARCH ARTICLE

Fatty acid receptor modulator PBI-4050 inhibits kidney fibrosis and improves glycemic control

Yan Li,[1,2,3] Sungjin Chung,[1,2] Zhilian Li,[1,2] Jessica M. Overstreet,[1,2] Lyne Gagnon,[4] Brigitte Grouix,[4] Martin Leduc,[4] Pierre Laurin,[4] Ming-Zhi Zhang,[1,2] and Raymond C. Harris[1,2,5]

[1]Division of Nephrology and Hypertension, Department of Medicine, and [2]Vanderbilt Center for Kidney Disease, Vanderbilt University School of Medicine, Nashville, Tennessee, USA. [3]Shanghai Ninth People's Hospital, Shanghai JiaoTong University School of Medicine, Shanghai, China, [4]Prometic BioSciences Inc., Laval, Quebec, Canada. [5]Department of Veterans Affairs, Nashville, Tennessee, USA.

Extensive kidney fibrosis occurs in several types of chronic kidney diseases. PBI-4050, a potentially novel first-in-class orally active low–molecular weight compound, has antifibrotic and antiinflammatory properties. We examined whether PBI-4050 affected the progression of diabetic nephropathy (DN) in a mouse model of accelerated type 2 diabetes and in a model of selective tubulointerstitial fibrosis. eNOS$^{-/-}$ *db/db* mice were treated with PBI-4050 from 8–20 weeks of age (early treatment) or from 16–24 weeks of age (late treatment). PBI-4050 treatment ameliorated the fasting hyperglycemia and abnormal glucose tolerance tests seen in vehicle-treated mice. In addition, PBI-4050 preserved (early treatment) or restored (late treatment) blood insulin levels and increased autophagy in islets. PBI-4050 treatment led to significant improvements in lifespan in the diabetic mice. Both early and late PBI-4050 treatment protected against progression of DN, as indicated by reduced histological glomerular injury and albuminuria, slow decline of glomerular filtration rate, and loss of podocytes. PBI-4050 inhibited kidney macrophage infiltration, oxidative stress, and TGF-β–mediated fibrotic signaling pathways, and it also protected against the development of tubulointerstitial fibrosis. To confirm a direct antiinflammatory/antifibrotic effect in the kidney, further studies with a nondiabetic model of EGFR-mediated proximal tubule activation confirmed that PBI-4050 dramatically decreased the development of the associated tubulointerstitial injury and macrophage infiltration. These studies suggest that PBI-4050 attenuates development of DN in type 2 diabetes through improvement of glycemic control and inhibition of renal TGF-β–mediated fibrotic pathways, in association with decreases in macrophage infiltration and oxidative stress.

Introduction

Free fatty acids (FFAs) are essential nutrients but have also been implicated in disease processes, including renal disease (1) and especially diabetic nephropathy (2). It is now recognized that FFAs can activate a family of cell-surface GPCRs. We have recently identified a compound — PBI-4050 (3-pentylbenzenacetic acid sodium salt), a synthetic analogue of a medium–chain length fatty acid — that binds to FFA receptor 1 (FFAR1/GPR40) and GPR84 (3). GPR40 and GPR84 show distinct characteristics both in fatty acid binding and in biological effects. GPR40 is activated by both medium- and long-chain FFAs (4), while GPR84 is responsive to medium-chain FFAs only (5).

GPR40 and GPR84 have distinct tissue expression profiles. GPR40 was initially identified to be expressed in pancreatic β cells and has been shown to enhance glucose-mediated insulin secretion (4). However, it has subsequently been found to have a broader expression pattern, including enteroendocrine cells of the gastrointestinal tract (6, 7), skin (8), nerves (9), and kidney tubules (10). In contrast, GPR84 is highly expressed on immune cells, including T and B cells (11), and granulocytes/monocytes/macrophages (5, 12), with upregulation in response to inflammation. GPR84 expression has also been reported in brain, heart, muscle, colon, thymus, spleen, kidney, liver, intestine, placenta, and lung, although cellular localization has not been performed. GPR84 expression in macrophages can prevent adiponectin release from adipocytes and therefore lead to fatty acid release (13).

Conflict of interest: The authors have declared that no conflict of interest exists.

Submitted: February 5, 2018
Accepted: April 13, 2018
Published: May 17, 2018

Reference information:
JCI Insight. 2018;3(10):e120365.
https://doi.org/10.1172/jci.insight.120365.

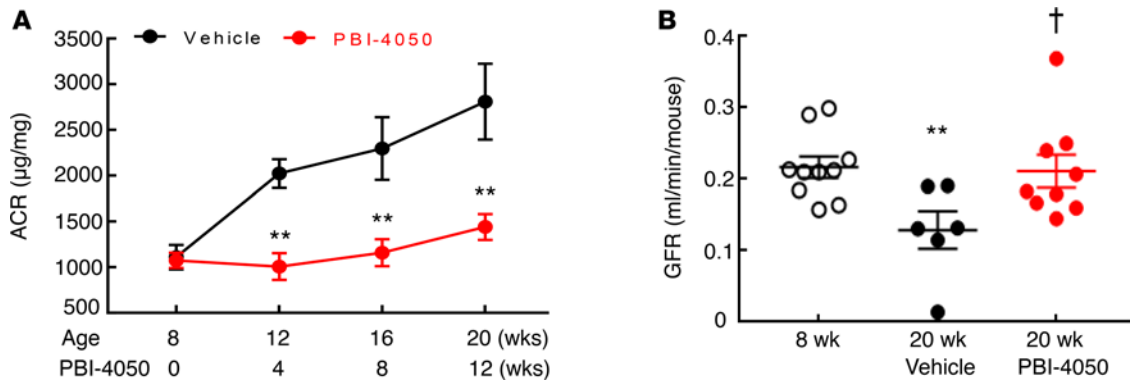

Figure 1. Effect of PBI-4050 treatment on albuminuria and glomerular filtration rate (GFR). (**A**) PBI-4050 treatment prevented the gradual increase in albuminuria seen in vehicle-treated eNOS$^{-/-}$ *db/db* mice from 8–20 weeks of age. $^{**}P < 0.01$ vs. corresponding vehicle group at the same time point; n = 12 in vehicle group and n = 10 in PBI-4050. (**B**) From 8–20 weeks of age, GFR markedly decreased in vehicle-treated eNOS$^{-/-}$ *db/db* mice but was stable in PBI-4050–treated eNOS$^{-/-}$ *db/db* mice, with higher GFR in PBI-4050 group than in vehicle group at 20 weeks of age. $^{**}P < 0.01$ vs. baseline; †$P < 0.05$ vs. vehicle group at 20 weeks of age; n = 10 in baseline group, n = 6 in vehicle group, n = 9 in PBI-4050 group. All values are shown as mean ± SEM. P values were calculated by Student's t test in **A** and by ANOVA and Bonferroni's t test in **B**.

Our recent studies have determined that PBI-4050 acts as an agonist for GPR40 and as an antagonist or inverse agonist for GPR84, and it inhibits fibrosis in a number of models of tissue fibrosis (3). In the present study, we determined the effect of treatment with this compound on progression of kidney injury in an accelerated model of diabetic nephropathy.

Results

To determine the potential role of PBI-4050 on diabetic kidney disease, we utilized an accelerated model of type 2 diabetic nephropathy, eNOS$^{-/-}$ *db/db* mice. In our initial studies, we treated mice with either vehicle or PBI-4050 (100 mg/kg) by daily gavage from 8–20 weeks of age. eNOS$^{-/-}$ *db/db* mice are moderately hypertensive (14, 15), and PBI-4050 had no effect on blood pressure (Supplemental Figure 1A; supplemental material available online with this article; https://doi.org/10.1172/jci.insight.120365DS1). In addition, there was no effect on body weight with PBI-4050 administration compared with vehicle-treated mice (Supplemental Figure 1B). By 8 weeks of age, the eNOS$^{-/-}$ *db/db* mice had already developed significant albuminuria, which progressively increased until 20 weeks of age in vehicle-treated mice (Figure 1A). In contrast, PBI-4050 prevented any further increase in albuminuria over the treatment period. Furthermore, compared with vehicle-treated mice, which exhibited a decrease in glomerular filtration rate (GFR) from 8–20 weeks, PBI-4050 preserved GFR (Figure 1B). Histological analysis indicated marked decreases in glomerulosclerosis (Figure 2A) and interstitial fibrosis (Figure 2B) in the PBI-4050–treated mice compared with vehicle-treated mice. Podocyte number per glomerulus section markedly decreased from 8–20 weeks of age in vehicle-treated mice, while PBI-4050 treatment significantly slowed this loss (Figure 2B).

To determine the effect of PBI-4050 in established diabetic nephropathy, we performed further studies in which we did not initiate therapy in eNOS$^{-/-}$ *db/db* mice until 16 weeks of age, a time at which the mice had already developed substantial glomerulopathy. As a comparator, we treated a subset of mice with the angiotensin-converting enzyme (ACE) inhibitor captopril, with or without concomitant administration of PBI-4050. As with earlier initiation of treatment, administration of PBI-4050 at 16 weeks of age did not affect body weight (Supplemental Figure 2). However, it did prevent further increases in albuminuria, while captopril led to a gradual decline in albuminuria. Of interest, the combination of PBI-4050 and captopril induced a marked early and sustained decrease in albuminuria (Figure 3A). Even with the delayed initiation of treatment with PBI-4050, there was a clear decrease in glomerulosclerosis and tubule injury at 24 weeks compared with vehicle-treated mice (Figure 3B), with reduced collagen deposition, as indicated by Masson's trichrome and Picrosirius red staining (Figure 3, C and D). A decrease in collagens I an IV expression was also observed by IHC, along with reductions in the myofibroblast marker smooth muscle actin α (α-SMA) and the profibrotic marker connective tissue growth factor (CTGF) (Figure 4A). Furthermore, phosphorylation of SMAD3, which results

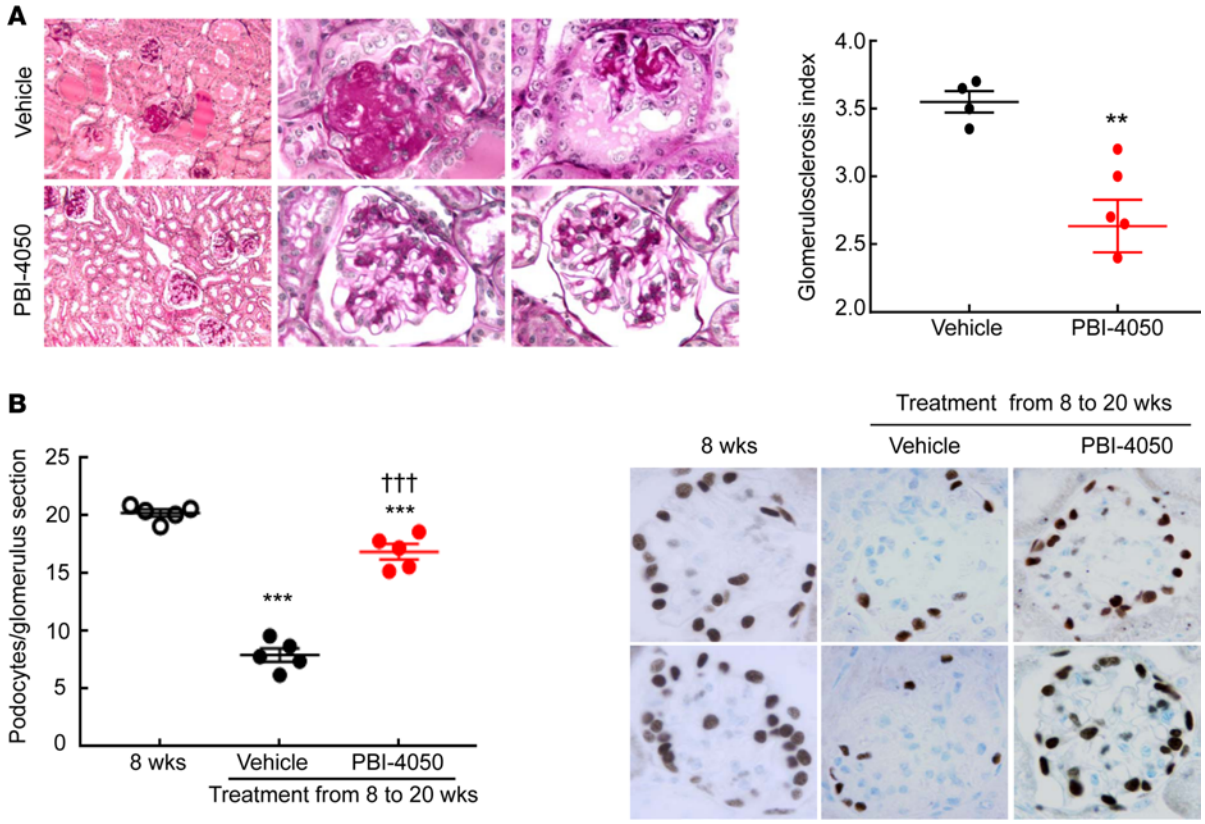

Figure 2. PBI-4050 attenuated diabetic nephropathy (DN) and slowed loss of podocytes. (**A**) PBI-4050 treatment attenuated glomerular injury in eNOS$^{-/-}$ *db/db* mice. $^{**}P < 0.01$; $n = 4$ in vehicle-treated eNOS$^{-/-}$ *db/db* mice and $n = 6$ in PBI-4050–treated eNOS$^{-/-}$ *db/db* mice. Original magnification, ×400. (**B**) Podocyte number/glomerulus section was significantly higher in PBI-4050–treated eNOS$^{-/-}$ *db/db* mice than vehicle-treated eNOS$^{-/-}$ *db/db* mice when the mice were sacrificed at 20 weeks of age. $^{***}P < 0.001$ vs. baseline, $^{†††}P < 0.001$ vs. vehicle group at 20 weeks of age; $n = 5$ in each group. Original magnification, ×400. PBI-4050 treatment attenuated tubulointerstitial fibrosis in eNOS$^{-/-}$ *db/db* mice as shown by Masson's trichrome staining. Original magnification: Left, ×100; middle and right lane, ×400. All values are shown as mean ± SEM. *P* values were calculated by Student's *t* test in **A**, and by ANOVA and Bonferroni's *t* test in **B**.

from activation of TGF-β, was significantly reduced by PBI-4050 (Figure 4B). There was also decreased renal macrophage infiltration with PBI-4050 (Figure 5A) and evidence for reduced oxidative stress, as indicated by decreased nitrotyrosine staining (Figure 5B).

As noted above, PBI-4050 acts as an agonist for GPR40 and as an antagonist for GPR84. In addition to its expression in the kidney, GPR40 is highly expressed in the pancreatic islets and has been reported to stimulate insulin release (16). Hence, we examined blood glucose in eNOS$^{-/-}$ *db/db* mice treated with PBI-4050 from 8–20 weeks. Compared with vehicle-treated mice, hyperglycemia was markedly decreased with PBI-4050 (Figure 6A), and glucose tolerance was markedly improved (Figure 6B). In mice in which PBI-4050 treatment was not initiated until 16 weeks, blood glucose still decreased compared with vehicle-treated mice (Figure 6C).

The *db/db* mice on the C57BLKS/J (BKS) background have been reported to develop progressive pancreatic isletitis and decreased insulin production (17). We confirmed progressive decrease in plasma insulin levels in vehicle-treated eNOS$^{-/-}$ *db/db* mice (Figure 7A). In contrast, when the mice were treated with PBI-4050 beginning at 8 weeks of age, there was preservation of plasma insulin levels (Figure 7B), while initiation of treatment at 16 weeks of age reverted plasma insulin levels toward levels seen at 8 weeks (Figure 7C). In these mice, PBI-4050 treatment resulted in a significant preservation of insulin expression in pancreatic islets at 24 weeks compared with vehicle-treated mice (Figure 7D), along with markedly decreased pancreatic fibrosis (Figure 8A). Since PBI-4050 is also an antagonist or inverse agonist of the proinflammatory GPR84, we examined its effects on islet inflammation and found a marked decrease in infiltration of both macrophages and CD8$^+$ T cells (Figure 8, B and C). There was decreased expression of the ER stress marker CHOP (Supplemental Figure 3), as well as an increase of autophagic activity in islets

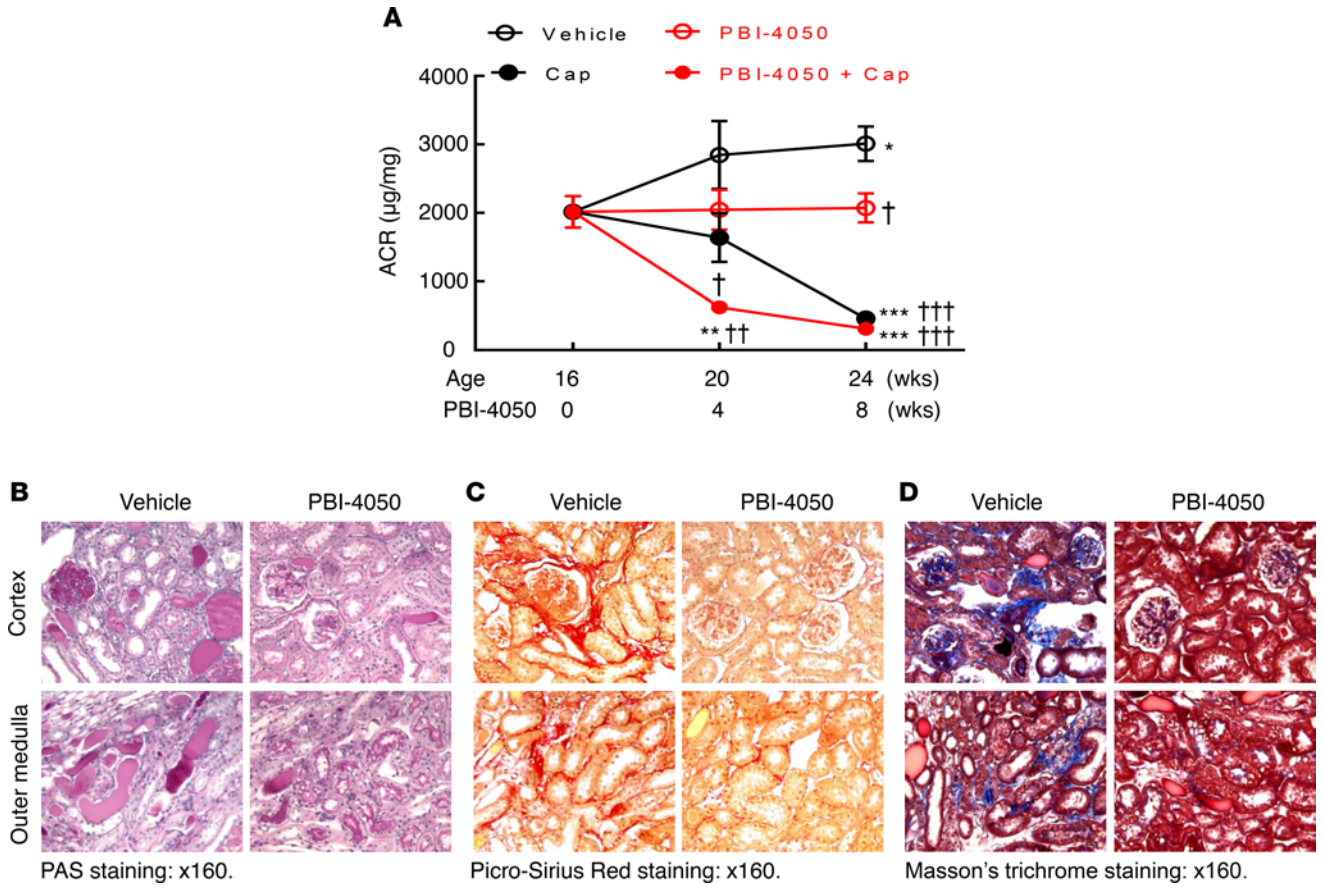

Figure 3. Late PBI-4050 treatment attenuated progression of diabetic nephropathy (DN) and had an additive effect with the angiotensin-converting enzyme inhibitor, captopril. (**A**) PBI-4050 treatment alone prevented further increases in albuminuria seen in vehicle-treated eNOS$^{-/-}$ *db/db* mice from 16–24 weeks of age, while it accelerated the reduction of albuminuria seen in eNOS$^{-/-}$ *db/db* mice treated with captopril. *P < 0.05, **P < 0.01, *** P < 0.001 vs. baseline (16 weeks of age); †P < 0.05, ††P < 0.01, †††P < 0.001 vs. corresponding vehicle group. n = 8 in each group. (**B**) There was less injury in both cortex and outer medulla in late PBI-4050–treated eNOS$^{-/-}$ *db/db* mice compared with vehicle-treated eNOS$^{-/-}$ *db/db* mice. (**C** and **D**) Late PBI-4050 treatment led to reduction in fibrosis in both cortex and outer medulla in eNOS$^{-/-}$ *db/db* mice, as indicated by Picro-sirius red staining (**C**) and Masson's trichrome staining (**D**). Original magnification, ×160 in all. All values are shown as mean ± SEM. All P values were calculated by ANOVA and Bonferroni's t test.

from PBI-4050–treated mice, as indicated by decreased expression of p62 (Figure 9). Finally, in addition to preservation of pancreatic islets, PBI-4050 markedly decreased hepatic steatosis in the eNOS$^{-/-}$ *db/db* mice (Supplemental Figure 4).

eNOS$^{-/-}$ *db/db* mice have a reduced lifespan and normally die between 24 and 28 weeks of age (18). We studied a subset of eNOS$^{-/-}$ *db/db* mice in which treatment with PBI-4050 or vehicle was initiated at 16 weeks. Compared with the 8 vehicle-treated mice, who had all died within 10 weeks, 6 of 8 PBI-4050–treated mice were still alive and appeared healthy after 14 weeks, when the experiment was terminated (Figure 10).

We have previously described a model of spontaneous tubulointerstitial fibrosis resulting from the selective overexpression of the EGFR ligand, HB-EGF, in renal proximal tubules (hHB-EGF$^{Tg/Tg}$) (19). These mice have augmented interstitial myofibroblast accumulation and progressive increase in interstitial extracellular matrix deposition. Because there are no apparent systemic metabolic abnormalities in these mice during the development of tubulointerstitial fibrosis, we tested whether PBI-4050 could affect the inexorable progression of the tubulointerstitial fibrosis in this nondiabetic model.

Our previous studies indicated an important role for EGFR-mediated ERK activation in induction of tubulointerstitial fibrosis (20), and treatment of hHB-EGF$^{Tg/Tg}$ mice with a MEK inhibitor to inhibit ERK activation attenuated development of the tubulointerstitial fibrosis (19). In the present studies, we found that PBI-4050 significantly decreased phospho-ERK overexpression seen in proximal tubules of the vehicle-treated mice (Figure 11A).

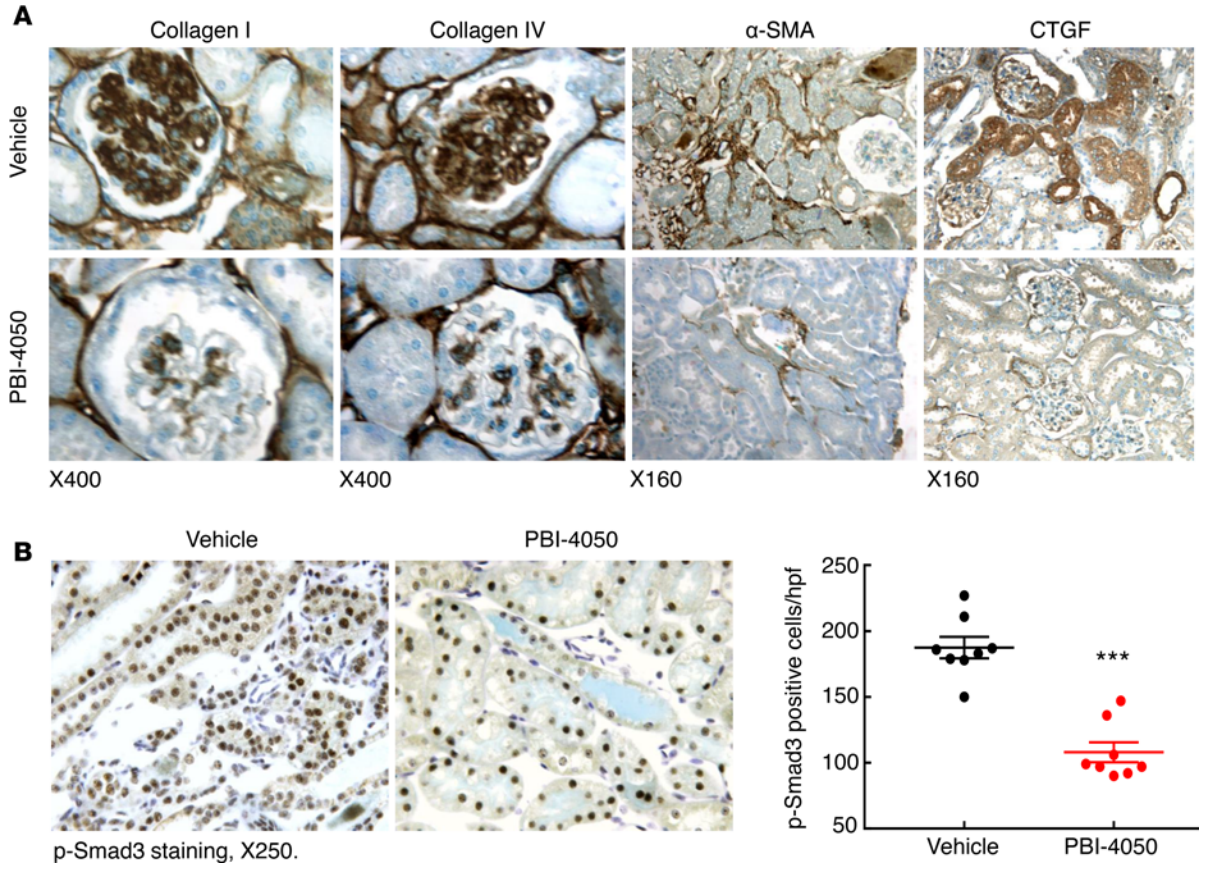

Figure 4. PBI-4050 treatment decreased mediators of renal fibrosis. (**A**) Immunostaining indicates that PBI-4050 treatment from 8–20 weeks of age reduced renal expression of profibrotic and fibrotic components including collagen I, collagen IV, α-SMA (marker of myofibroblasts), and connective tissue growth factor (CTGF) in eNOS$^{-/-}$ *db/db* mice. Original magnification, ×160 in all. (**B**) PBI-4050 treatment inhibited renal expression levels of phospho-Smad3, an indicator of activation of the TGF-β signaling pathway in eNOS$^{-/-}$ *db/db* mice. ***$P < 0.001$ vs. vehicle; $n = 8$ in each group. Original magnification, ×250. All values are shown as mean ± SEM. *P* value was calculated by Student's *t* test.

Accumulation of extracellular matrix is the pathological hallmark of tubulointerstitial fibrosis. Sustained EGFR activation in the proximal tubule in the vehicle-treated hHB-EGF$^{Tg/Tg}$ mice induced significant collagen deposition by 15 weeks, as indicated by Picrosirius red staining (Figure 11B). In contrast, PBI-4050 administration markedly decreased tubulointerstitial fibrosis. PBI-4050 treatment also resulted in decreased mRNA expression of collagen I, the myofibroblast marker; α-SMA; the profibrotic cytokines TGF-β and CTGF; and the extracellular matrix component, fibronectin (Figure 11C). Immunoblotting and immunostaining confirmed PBI-4050–mediated decreases in α-SMA and fibronectin protein levels, as well as decreased phosphorylation of SMAD3 (Figure 11, A and C).

There is increasing evidence that tubular dysfunction contributes to the initiation and progression of fibrosis, and that when renal epithelial cells revert to a dedifferentiated state, they produce profibrotic and proinflammatory cytokines. A number of markers of epithelial dedifferentiation have been described, including decreased expression of the adherens junction protein E-cadherin and increased expression of the transcription factors Snail1 and Snail2. In this regard, compared with vehicle-treated hHB-EGF$^{Tg/Tg}$ mice, PBI-4050–treated mice had relative preservation of E-cadherin expression and inhibition of Snail2 expression (Figure 12, A and B). Furthermore, there was a marked decrease in renal interstitial macrophage infiltration in the PBI-4050–treated mice (Figure 12C), in accordance with results seen in the eNOS$^{-/-}$ *db/db* mice (Figure 5A).

Discussion

These studies examined the effect of PBI-4050, a dual GPR40/GPR84 antagonist, on the progression of kidney injury in an accelerated mouse model of type 2 diabetic nephropathy. In this robust model, PBI-4050 decreased blood glucose and improved glucose tolerance. In addition, it led to decreased pancreatic islet

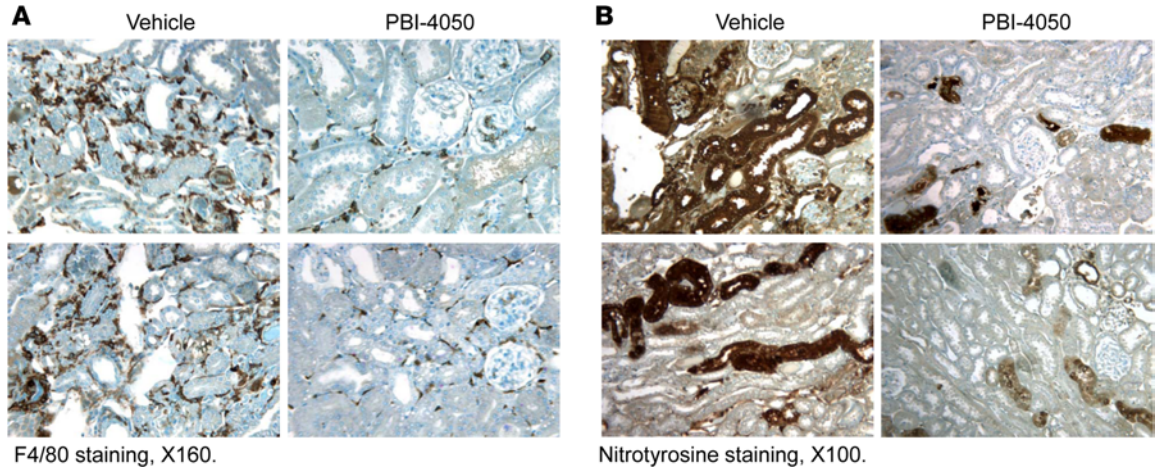

Figure 5. PBI-4050 treatment inhibited renal macrophage infiltration and oxidative stress. (**A**) PBI-4050 treatment from 8–20 weeks of age suppressed renal macrophage infiltration, as indicated by reduction in F4/80 staining (marker of macrophages) in eNOS$^{-/-}$ *db/db* mice. (**B**) PBI-4050 treatment also inhibited renal oxidative stress as indicated by decreased nitrotyrosine staining, a marker of oxidative stress. Original magnification, ×160 in **A**; ×100 in **B**.

inflammation and preservation of β cell expression of insulin. It also reduced both functional and structural glomerulopathy. To confirm a direct antiinflammatory/antifibrotic effect in the kidney, further studies with a nondiabetic model of EGFR-mediated proximal tubule activation confirmed that PBI-4050 dramatically decreased the development of the associated tubulointerstitial injury

One important finding in this study is that PBI-4050 protected against podocyte loss. In the current study, we counted WT-positive nuclei in 4-μm thick sections as podocyte number per cross section, which gives relative podocyte density in different groups. We are aware that, for absolute podocyte count/per glomerulus, there are advantages to utilize classical podocyte morphometry studies described by Basgen's group (21).

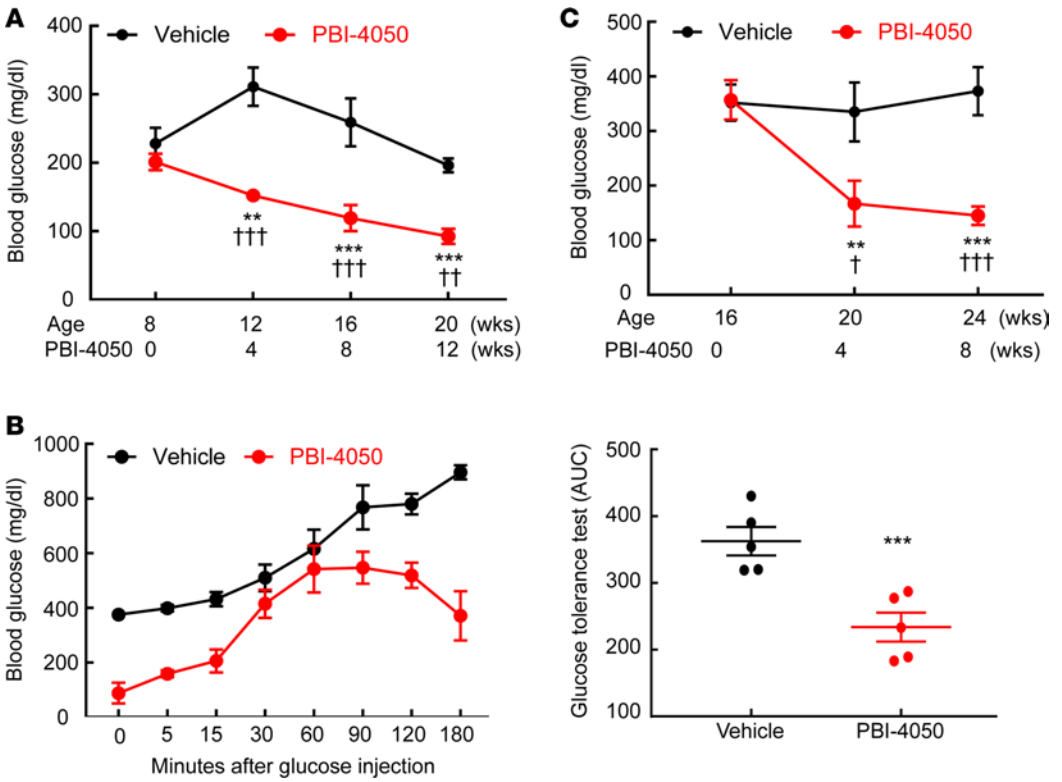

Figure 6. PBI-4050 treatment decreased blood glucose and increased glucose tolerance. (**A**) PBI-4050 treatment from 8–20 weeks of age led to a gradual decrease in fasting blood glucose in eNOS$^{-/-}$ *db/db* mice. $^{**}P < 0.01$, $^{***}P < 0.001$ vs. baseline; $^{††}P < 0.01$, $^{†††}P < 0.001$ vs. corresponding vehicle group. $n = 10$ in each group. (**B**) PBI-4050 increased glucose tolerance at the end of treatment from 0–180 minutes. $^{***}P < 0.001$ vs. vehicle group; $n = 5$ in each group. (**C**) Late PBI-4050 treatment from 16–24 weeks of age also decreased blood glucose. $^{**}P < 0.01$, $^{***}P < 0.001$ vs. baseline; $^{†}P < 0.05$, $^{†††}P < 0.001$ vs. corresponding vehicle group; $n = 6$ in each group. All values are shown as mean ± SEM. All *P* values were calculated by ANOVA and Bonferroni's *t* test in **A** and **C**, and by Student's *t* test in **B**.

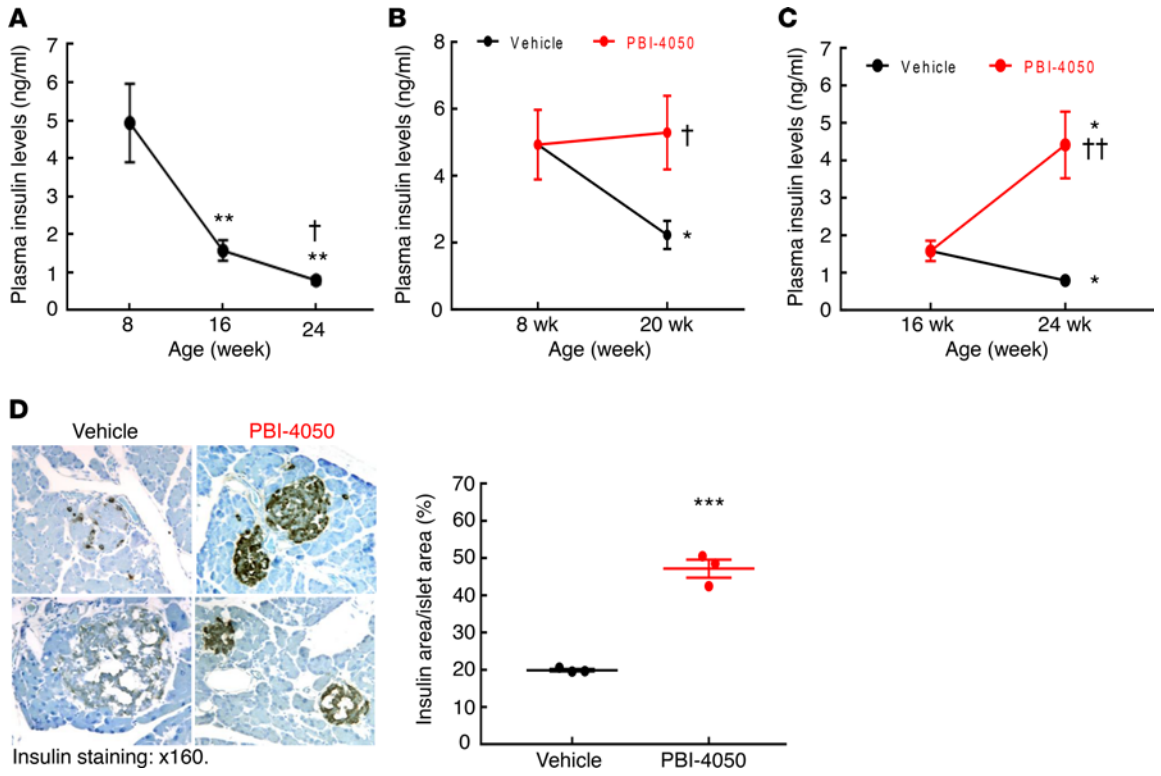

Figure 7. PBI-4050 treatment protected insulin production. (**A**) Plasma insulin levels in vehicle-treated eNOS$^{-/-}$ *db/db* mice progressively decreased from 8–24 weeks of age. $^{**}P < 0.01$ vs. 8 weeks of age; †$P < 0.05$ vs. 16 weeks of age; $n = 4$ in each group. (**B**) PBI-4050 treatment from 8–20 weeks of age preserved plasma insulin levels in eNOS$^{-/-}$ *db/db* mice. $^{*}P < 0.05$ vs. 8 weeks of age; †$P < 0.05$ vs. corresponding vehicle group; $n = 4$ in each group. (**C**) Late PBI-4050 treatment of eNOS$^{-/-}$ *db/db* mice from 16–24 weeks of age restored plasma insulin levels to levels seen at 8 weeks of age. $^{*}P < 0.05$ vs. 16 weeks of age; ††$P < 0.01$ vs. corresponding vehicle group; $n = 4$ in each group. (**D**) Insulin immunostaining indicated higher levels of insulin expression in islets from PBI-4050–treated eNOS$^{-/-}$ *db/db* mice. $^{***}P < 0.001$, $n = 3$ in each group. Original magnification, ×160. All values are shown as mean ± SEM. All *P* values were calculated by ANOVA and Bonferroni's *t* test in **A–C** and by Student's *t* test in **D**.

Our previous studies demonstrated that a significant component of the beneficial effect of RAS inhibition in the eNOS$^{-/-}$ *db/db* model was due to decreases in blood pressure (14) but that there was no protection against podocyte loss (22). In contrast, PBI-4050 did not decrease hypertension (Supplemental Figure 1) but did protect against podocyte loss (Figure 2), suggesting a different method of action and raising the possibility of additive protective effects of PBI-4050 and RAS inhibitors.

The beneficial effect of PBI-4050 in 2 distinct models of progressive kidney fibrosis indicates the importance of these fatty acid–activated GPCRs in the mediation of kidney injury. We have previously shown that GPR40 is protective, while GPR84 is deleterious in kidney fibrosis, as observed with a significant increase of fibrosis in GPR40-null mice and reduction of fibrosis in GPR84-null mice (3). Our previous studies indicated that GPR40 is expressed in the mouse kidney, with the highest expression in the cortex and outer stripe of the outer medulla, and is most highly expressed in the epithelia (10). In contrast, GPR84 is abundantly found in monocytes/macrophages, granulocytes, and neutrophils, and it has been reported to mediate inflammatory cell activation (5,15, 23). It is notable that there was markedly decreased inflammatory infiltrate following PBI-4050 treatment in renal tissue of both models of kidney injury. Furthermore, the islets of the PBI-4050–treated eNOS$^{-/-}$ *db/db* mice had decreased fibrosis and decreased T cell and macrophage infiltration, consistent with the prevention of the observed isletitis and decreased insulin expression and secretion that is known to occur in *db/db* mice on the BKS background (17). In addition, there was decreased hepatic steatosis with PBI-4050. These findings suggest that PBI-4050 might also have a beneficial effect to prevent adipose inflammation, although further studies will be required to confirm this hypothesis.

The preclinical findings presented here suggest that PBI-4050 may have broad applicability as a therapeutic option for many fibrosing conditions. In this regard, significant clinical activity observed in recent

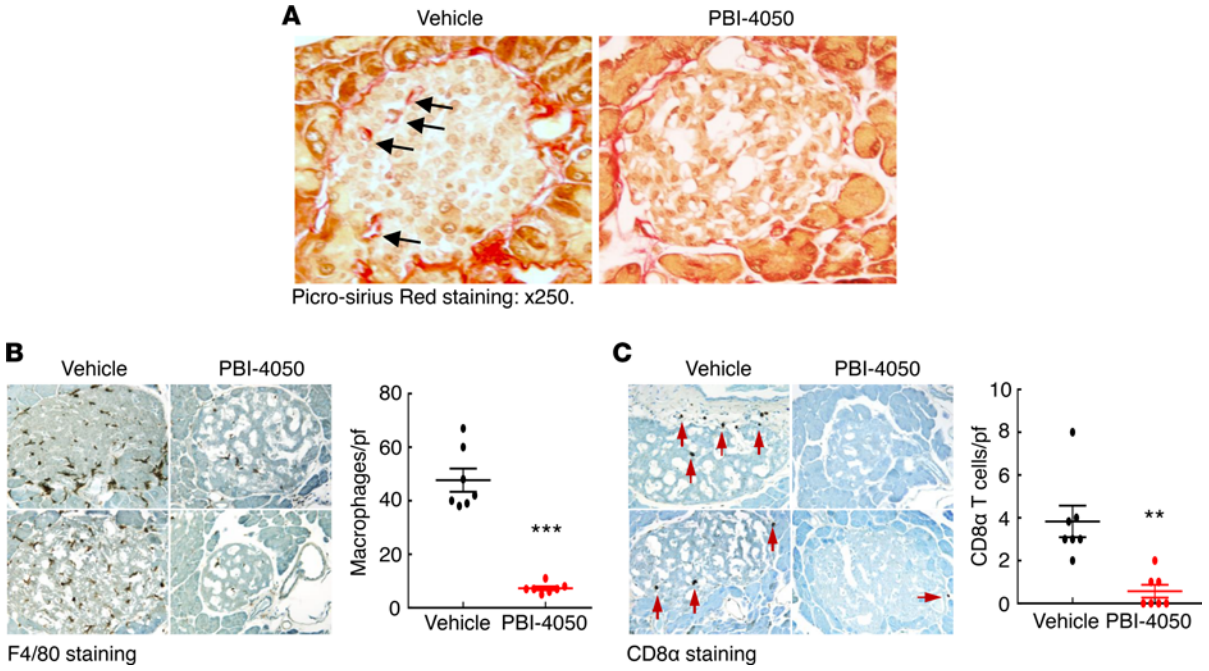

Figure 8. PBI-4050 treatment decreased fibrosis and leukocyte infiltration in pancreas. (**A**) PBI-4050 reduced fibrosis in pancreas islets in eNOS$^{-/-}$ *db/db* mice as shown by Picrosirius red staining; arrows show fibrotic areas. (**B**) Islet macrophage density was markedly lower in PBI-4050–treated eNOS$^{-/-}$ *db/db* mice compared with vehicle-treated eNOS$^{-/-}$ *db/db* mice as indicated by F4/80 staining. ***$P < 0.001$, $n = 7$ in each group. (**C**) Islet cytotoxic CD8 lymphocyte density was significantly lower in PBI-4050–treated eNOS$^{-/-}$ *db/db* mice compared with vehicle-treated eNOS$^{-/-}$ *db/db* mice. Arrows indicate CD8α^{+} cells. **$P < 0.01$, $n = 7$ in each group. Original magnification, ×250 in all. All values are shown as mean ± SEM. All *P* values were calculated by Student's *t* test.

phase 2 clinical trials in type 2 diabetes subjects with metabolic syndrome (24), in idiopathic pulmonary fibrosis patients (25), and in Alström syndrome patients (a rare syndrome characterized by obesity, type 2 diabetes, dyslipidemia, hypertension, and severe multiorgan fibrosis involving the liver, kidney, and heart) confirm translation of pharmacological activity of PBI-4050 in humans. Of interest, PBI-4050 has been well tolerated and shown to demonstrate a good safety profile in these early-phase clinical trials. In addition, in our current preclinical study, PBI-4050 treatment for 12 weeks had no effects on blood pressure, body weight, or animal physical activity, and all mice survived for the entire experimental period. As we do not have information regarding PBI-4050 crossing the blood brain barrier, its effect on the brain cannot be excluded.

In summary, these results suggest that PBI-4050 protects against diabetic nephropathy, potentially through stimulation of renal GPR40 and inhibition of renal GPR84, leading to decreased immune cell infiltration, oxidative stress, and fibrosis inhibition. In addition, PBI-4050 may also directly stimulate islet GPR40 and inhibit inflammatory cell GPR84, leading to increased autophagy, decreased immune cell infiltration and ER stress, subsequent preservation of islet function, and decreased blood glucose.

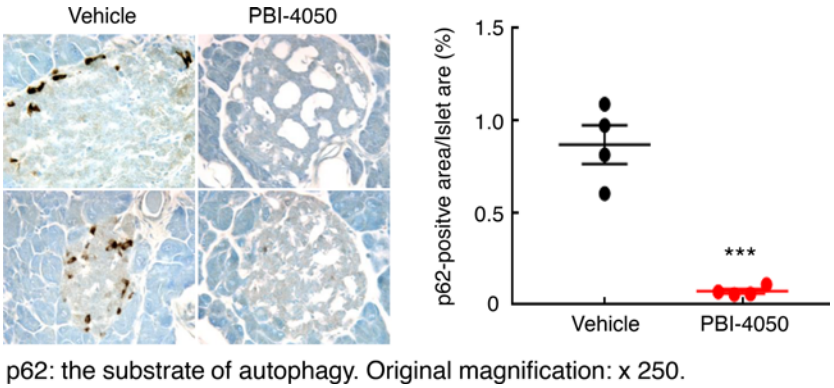

Figure 9. PBI-4050 treatment increased islet autophagy signaling. PBI-4050 treatment from 8–20 weeks of age in eNOS$^{-/-}$ *db/db* mice increased islet autophagy activity as indicated by decreased p62 expression, a substrate of autophagy. ***$P < 0.001$, $n = 4$ in each group. Original magnification, ×250. All values are shown as mean ± SEM. *P* value was calculated by Student's *t* test.

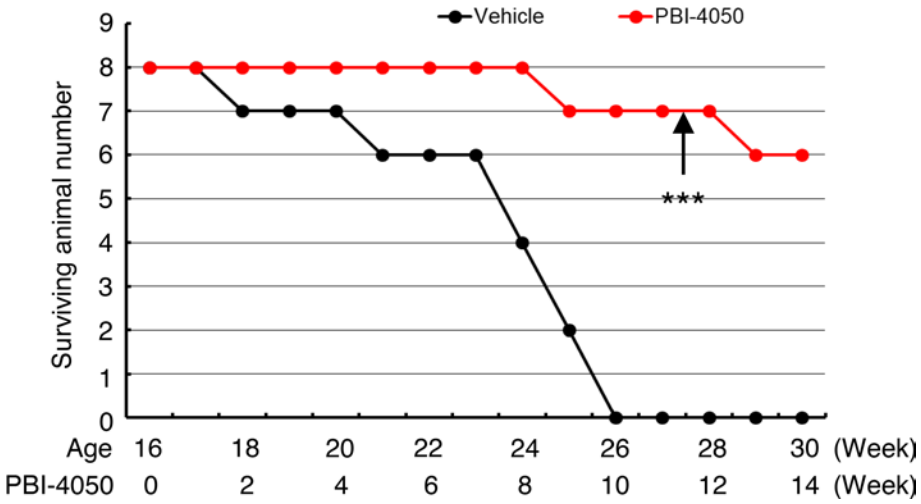

Figure 10. Late PBI-4050 treatment increased the survival of eNOS$^{-/-}$ *db/db* mice. Treatment of eNOS$^{-/-}$ *db/db* mice with PBI-4050 or vehicle was initiated at the age of 16 weeks and continued until 30 weeks. ***$P < 0.001$ vs. vehicle group, $n = 8$ in each group. Kaplan-Meier survival analysis and log-rank test were used.

Therefore, PBI-4050 may protect against diabetic nephropathy through both direct kidney protection and improved glucose tolerance secondary to islet protection.

Methods

Animal studies. Type 2 diabetes eNOS$^{-/-}$ *db/db* mice on the BKS background were generated as described previously (18). Genotyping was performed by PCR. A subset of eNOS$^{-/-}$ *db/db* male mice (8 weeks old) were randomized to 2 groups. One group was treated with PBI-4050 (100 mg/kg/day, $n = 10$), and the other group received vehicle (water, $n = 12$). Both PBI-4050 and water were given via daily gavage from 8–20 weeks. Mice were euthanized at 20 weeks of age. The second set of eNOS$^{-/-}$ *db/db* male mice were divided into 4 groups (8 mice in each group): vehicle (water), PBI-4050 (100 mg/kg/day; Prometic BioSciences Inc.), captopril (0.75 mg/ml in drinking water; Cayman Chemicals), and PBI-4050 plus captopril. The treatment was begun at 16 weeks and ended at 24 weeks. The third set of eNOS$^{-/-}$ *db/db* male mice was divided into 2 groups (8 mice in each group): vehicle (water) and PBI-4050 (100 mg/kg/day). The treatment began at 16 weeks and lasted up to 30 weeks or until death.

The previously described hHB-EGF$^{+/Tg}$ mice (26) were bred onto a C57BL/6 background, a relatively fibrosis-resistant mouse strain. The Cre recombinase controlled by the γ-glutamyl transpeptidase promoter (*γGT-Cre*) allows successful targeting of hHB-EGF expression to the renal proximal tubule. Gene expression usually commences 10–14 days postnatally. Male homozygous transgenic mice (hHB-EGF$^{Tg/Tg}$) were genotyped using PCR and used for subsequent experiments.

Measurements of glomerular filtration rate (GFR) in conscious mice. GFR was measured as we have reported previously (27). GFR was measured before initiation of the experiment (7–8 weeks of age) and at the end of the experiment (20 weeks of age).

Measurements of blood glucose, insulin, and urinary albumin excretion. Fasting blood glucose was evaluated with a B-glucose analyzer (HemoCue) in conscious mice on saphenous vein samples at 2:00 p.m. after fasting for 6 hours initiated at 8:00 a.m. Plasma insulin was measured through Vanderbilt Diabetes Research and Training Center using radioimmunoassay (RIA). Urinary albumin and creatinine excretion was determined using Albuwell M kits (Exocell). Albuminuria is expressed as urinary albumin concentration versus creatinine concentration ratio (ACR, μg/mg).

I.p. glucose tolerance test (IPGTT). Mice were fasted overnight (16 hours), 100 mg/ml glucose solution was injected i.p. at a dose of 2 mg/g body weight (200 μl/10 g body weight), and blood was collected and glucose level measured at 0, 15, 30, 90, 120, 150, and 180 minutes after injection.

Antibodies. Rat anti–mouse F4/80 (catalog MCA497R) and CD8α (catalog MCA2694) were purchased from Bio-Rad; rabbit anti–human fibronectin (catalog F3648) and mouse anti–α-SMA (a marker of myofibroblasts, catalog A5228) were from MilliporeSigma; rabbit anti–murine collagen type I (catalog 600-401-103-01),

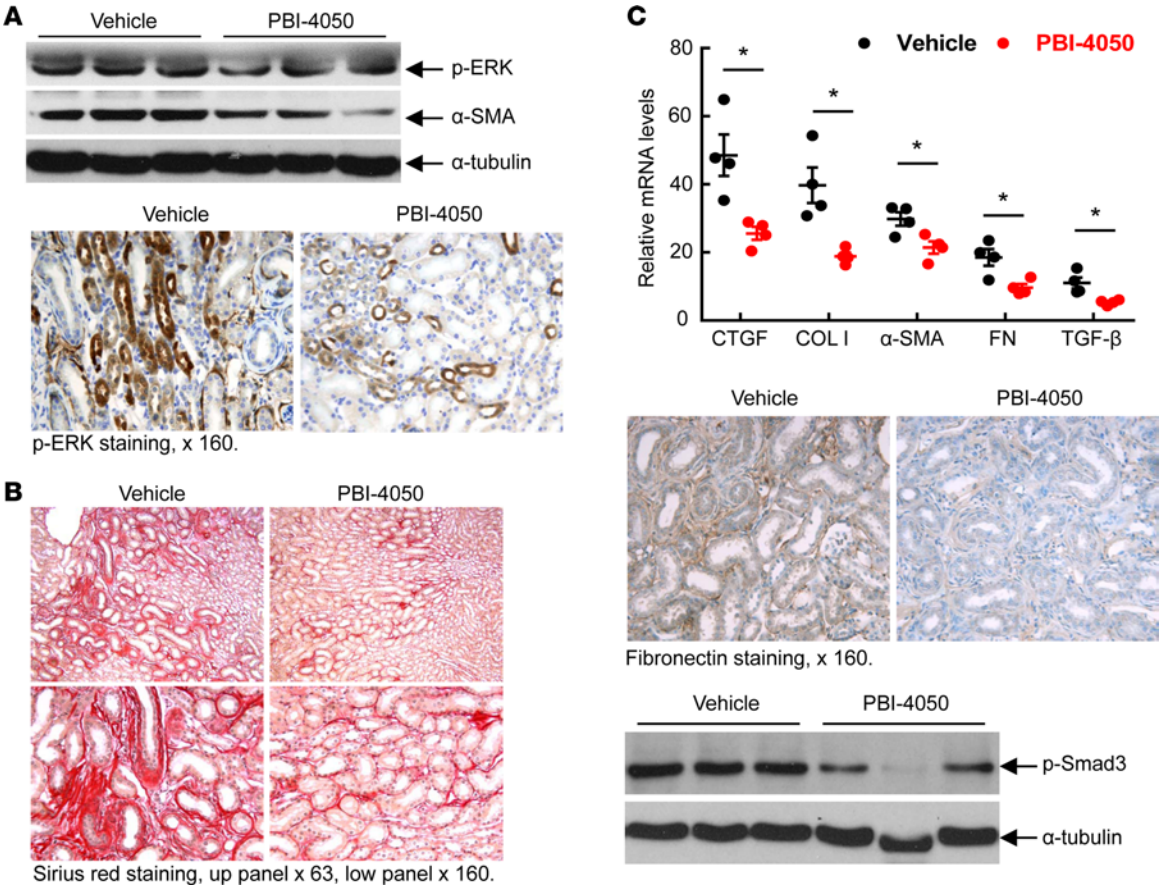

Figure 11. PBI-4050 treatment reduced renal interstitial fibrosis in hHB-EGF$^{Tg/Tg}$ fibrotic mice. (**A**) Reduction of EGFR-mediated renal ERK activation and α-SMA (marker of myofibroblasts) was evident in hHB-EGF$^{Tg/Tg}$ mice treated with PBI-4050 from 5–15 weeks of age. (**B**) Picrosirius red staining demonstrated decreased renal fibrosis in PBI-4050–treated hHB-EGF$^{Tg/Tg}$ mice. (**C**) PBI-4050 treatment reduced renal expression levels of profibrotic and fibrotic components including connective tissue growth factor (CTGF), collagen I, α-SMA, fibronectin, and TGF-β, as well as phosphorylation of SMAD3. *$P < 0.05$, $n = 4$. Original magnification, ×63 in the upper panels of **B**; ×160 in **A**, **C**, and lower panels of **B**. All values are shown as mean ± SEM. All P values were calculated by Student's t test.

collagen type IV (catalog 600-401-106-01), and p-smad3 (catalog 600-401-919) were from Rockland Immunochemicals; goat anti–human CTGF (catalog SC-14939) and rabbit anti–nitrotyrosine antibody (catalog SC-55256) were from Santa Cruz Biotechnology Inc.; rabbit anti–phospho-ERK and anti-p62 (catalog 5114), and mouse anti–C/EBP homologous protein (CHOP, catalog 2895) were from Cell Signaling Technology; guinea pig anti-insulin antibody (catalog ab7842), rabbit anti–Wilms Tumor Protein (WT1; catalog ab89901) and anti–E Cadherin (catalog ab15148), and goat anti-snail2 (catalog ab53519) were from Abcam.

RNA isolation and qPCR. Total RNAs from kidneys were isolated using TRIzol reagents (Invitrogen). qPCR was performed using TaqMan real-time PCR (7900HT, Applied Biosystems). The Master Mix and all gene probes were also purchased from Applied Biosystems. The probes used in the experiments included mouse S18 (Mm02601778), collagen I (Col1a1, Mm00801666), α-SMA (acta2, Mm01546133), fibronectin 1 (Fn1, Mm01256744), CTGF (Mm01192933), and TGF-β (Mm00441726).

Masson's trichrome staining and Picrosirius red staining. Masson's trichrome staining and Picrosirius red staining were performed according to the protocol provided by the manufacturer (MilliporeSigma).

IHC staining, quantitative image analysis, and immunoblotting. The animals were anesthetized with nembutal (70 mg/kg, i.p.; Abbott) and given heparin (1,000 units/kg, i.p.; Abbott) to minimize coagulation. The kidney was immersed in FPAS (3.7% formaldehyde, 10 mM sodium *m*-periodate, 40 mM phosphate buffer, and 1% acetic acid) for immunohistochemical staining. The fixed kidney was dehydrated through a graded series of ethanols, embedded in paraffin, sectioned (4 μm), and mounted on glass slides. Immunostaining was carried out as previously described (28). Based on the distinctive density and color of immunostaining in video images, the number, size, and position of stained cells were quantified using the BIOQUANT true- color windows

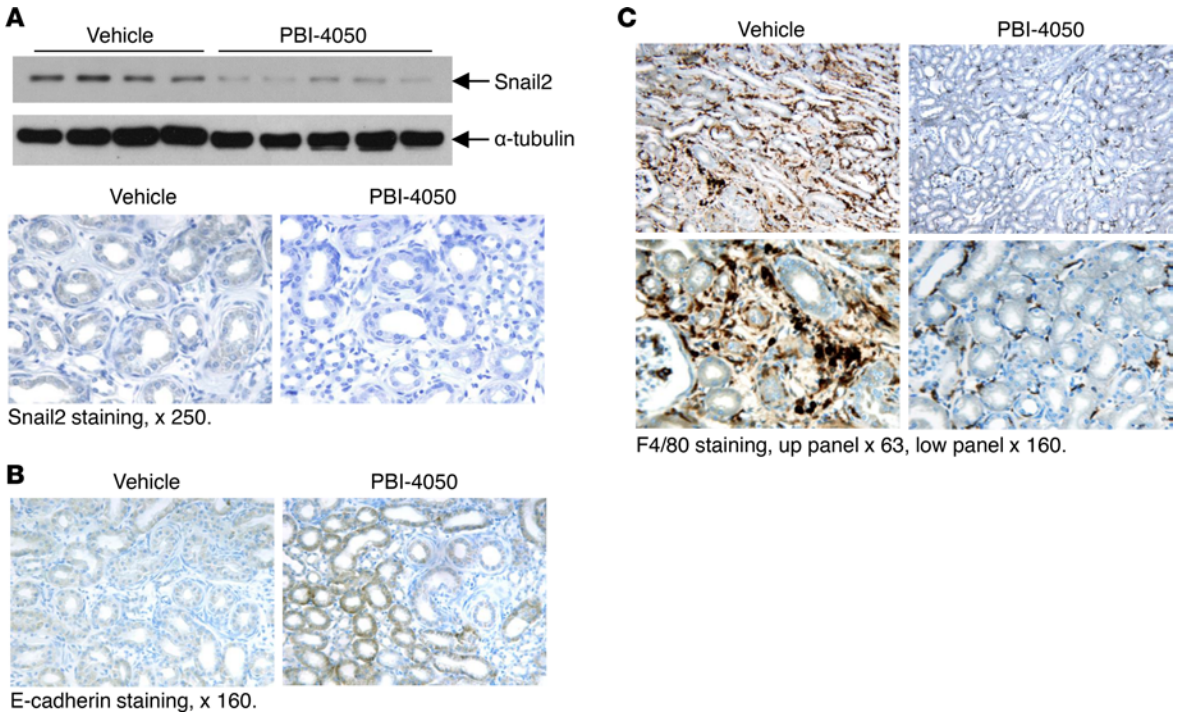

Figure 12. PBI-4050 treatment inhibited epithelial cell dedifferentiation and macrophage infiltration. (**A** and **B**) PBI-4050 treatment reduced renal Snail2 expression levels as indicated by immunoblotting and immunostaining (**A**) but increased the immunostaining of E-cadherin (**B**). (**C**) PBI-4050 treatment decreased renal macrophage infiltration in hHB-EGF$^{Tg/Tg}$ mice, as indicated by F4/80 staining. Original magnification, ×63 in the upper panels of **C**; ×160 in **B** and lower panels of **C**; ×250 in **A**. All values are shown as mean ± SEM. All *P* values were calculated by Student's *t* test.

system (R & M Biometrics) as previously described (29). Six representative fields from each animal were quantified, and their average was used as data from 1 animal sample. Immunoblotting was carried out as in previous reports (28).

Blood pressure measurement. Blood pressure was measured in awake mice with a tail-cuff microphonic manometer (30). In brief, mice were trained for 3 consecutive days at room temperature (Monday to Wednesday) before systolic blood pressure (SBP) was recorded during the following 2 days (Thursday and Friday) using a tail-cuff monitor (BP-2000 BP Analysis System, Visitech System). SBPs recorded on 2 consecutive days were averaged and used as SBP from 1 mouse.

Statistics. All values are presented as means, with data represented as ± SEM. Two-tailed Student's *t* tests, 2-way ANOVA, and Bonferroni's *t* tests were used for statistical analysis.

Study approval. All animal experiments were performed in accordance with the guidelines of the IACUC of Vanderbilt University.

Author contributions

YL, SC, ZL, JMO, MZZ, and RCH performed the studies; MZZ and RCH wrote the manuscript; and LG, BG, ML, and PL provided reagents and edited the manuscript.

Acknowledgments

This work was supported by NIH grants DK-95785, DK-51265, and DK-114809 (to MZZ and RCH); DK-62794 and DK-103067 (to RCH); and funds from the Department of Veterans Affairs (to RCH).

Address correspondence to: Raymond C. Harris, C-3321 Medical Center North, Department of Medicine, Vanderbilt University School of Medicine, Nashville, Tennessee 37232, USA. Phone: 615.322.2150; Email: ray.harris@vanderbilt.edu. Or to: Ming-Zhi Zhang, S3223 Medical Center North, Department of Medicine, Vanderbilt University School of Medicine, Nashville, Tennessee 37232, USA. Phone: 615.343.1548; Email: ming-zhi.zhang@vanderbilt.edu.

1. Kang HM, et al. Defective fatty acid oxidation in renal tubular epithelial cells has a key role in kidney fibrosis development. *Nat Med*. 2015;21(1):37–46.
2. Fan Y, Lee K, Wang N, He JC. The Role of Endoplasmic Reticulum Stress in Diabetic Nephropathy. *Curr Diab Rep*. 2017;17(3):17.
3. Gagnon L, et al. A Newly Discovered Antifibrotic Pathway Regulated by Two Fatty Acid Receptors: GPR40 and GPR84. *Am J Pathol*. 2018;188(5):1132–1148.
4. Itoh Y, et al. Free fatty acids regulate insulin secretion from pancreatic beta cells through GPR40. *Nature*. 2003;422(6928):173–176.
5. Wang J, Wu X, Simonavicius N, Tian H, Ling L. Medium-chain fatty acids as ligands for orphan G protein-coupled receptor GPR84. *J Biol Chem*. 2006;281(45):34457–34464.
6. Edfalk S, Steneberg P, Edlund H. Gpr40 is expressed in enteroendocrine cells and mediates free fatty acid stimulation of incretin secretion. *Diabetes*. 2008;57(9):2280–2287.
7. Liou AP, et al. The G-protein-coupled receptor GPR40 directly mediates long-chain fatty acid-induced secretion of cholecystokinin. *Gastroenterology*. 2011;140(3):903–912.
8. Fujita T, Matsuoka T, Honda T, Kabashima K, Hirata T, Narumiya S. A GPR40 agonist GW9508 suppresses CCL5, CCL17, and CXCL10 induction in keratinocytes and attenuates cutaneous immune inflammation. *J Invest Dermatol*. 2011;131(8):1660–1667.
9. Nakamoto K, et al. Dysfunctional GPR40/FFAR1 signaling exacerbates pain behavior in mice. *PLoS One*. 2017;12(7):e0180610.
10. Ma SK, Wang Y, Chen J, Zhang MZ, Harris RC, Chen JK. Overexpression of G-protein-coupled receptor 40 enhances the mitogenic response to epoxyeicosatrienoic acids. *PLoS One*. 2015;10(2):e0113130.
11. Venkataraman C, Kuo F. The G-protein coupled receptor, GPR84 regulates IL-4 production by T lymphocytes in response to CD3 crosslinking. *Immunol Lett*. 2005;101(2):144–153.
12. Tan JK, McKenzie C, Mariño E, Macia L, Mackay CR. Metabolite-Sensing G Protein-Coupled Receptors-Facilitators of Diet-Related Immune Regulation. *Annu Rev Immunol*. 2017;35:371–402.
13. Nagasaki H, et al. Inflammatory changes in adipose tissue enhance expression of GPR84, a medium-chain fatty acid receptor: TNFα enhances GPR84 expression in adipocytes. *FEBS Lett*. 2012;586(4):368–372.
14. Zhang MZ, et al. Role of blood pressure and the renin-angiotensin system in development of diabetic nephropathy (DN) in eNOS-/- db/db mice. *Am J Physiol Renal Physiol*. 2012;302(4):F433–F438.
15. Wang X, et al. Macrophage Cyclooxygenase-2 Protects Against Development of Diabetic Nephropathy. *Diabetes*. 2017;66(2):494–504.
16. Yamashima T. Dual effects of the non-esterified fatty acid receptor 'GPR40' for human health. *Prog Lipid Res*. 2015;58:40–50.
17. Cucak H, Grunnet LG, Rosendahl A. Accumulation of M1-like macrophages in type 2 diabetic islets is followed by a systemic shift in macrophage polarization. *J Leukoc Biol*. 2014;95(1):149–160.
18. Zhao HJ, et al. Endothelial nitric oxide synthase deficiency produces accelerated nephropathy in diabetic mice. *J Am Soc Nephrol*. 2006;17(10):2664–2669.
19. Overstreet JM, et al. Selective activation of epidermal growth factor receptor in renal proximal tubule induces tubulointerstitial fibrosis. *FASEB J*. 2017;31(10):4407–4421.
20. Chen J, et al. EGFR signaling promotes TGFβ-dependent renal fibrosis. *J Am Soc Nephrol*. 2012;23(2):215–224.
21. Nicholas SB, Basgen JM, Sinha S. Using stereologic techniques for podocyte counting in the mouse: shifting the paradigm. *Am J Nephrol*. 2011;33 Suppl 1:1–7.
22. Zhang MZ, et al. Lysophosphatidic Acid Receptor Antagonism Protects against Diabetic Nephropathy in a Type 2 Diabetic Model. *J Am Soc Nephrol*. 2017;28(11):3300–3311.
23. Suzuki M, et al. Medium-chain fatty acid-sensing receptor, GPR84, is a proinflammatory receptor. *J Biol Chem*. 2013;288(15):10684–10691.
24. Laurin P, Grouix B, Laverdure A, Zacharie B, Gagnon L. PBI-4050 reduces cardiovascular and renal biomarkers in type II diabetic patients with metabolic syndrome. Prometic Biosciences Inc. http://www.prometic.com/wp-content/uploads/2017/02/PosterAHA2016_LG-final-002-002.pdf. Accessed April 25, 2018.
25. Parker J. PBI-4050 is Safe and Well Tolerated and Shows Evidence of Benefit in Idiopathic Pulmonary Fibrosis. Prometic Biosciences Inc. http://www.prometic.com/wp-content/uploads/2017/05/PBI-4050-IPF-P2-ATS-oral-presentation-07-May-2017-Final.pdf. Accessed April 25, 2018.
26. Zhang MZ, et al. CSF-1 signaling mediates recovery from acute kidney injury. *J Clin Invest*. 2012;122(12):4519–4532.
27. Qi Z, et al. Serial determination of glomerular filtration rate in conscious mice using FITC-inulin clearance. *Am J Physiol Renal Physiol*. 2004;286(3):F590–F596.
28. Zhang MZ, Wang Y, Paueksakon P, Harris RC. Epidermal growth factor receptor inhibition slows progression of diabetic nephropathy in association with a decrease in endoplasmic reticulum stress and an increase in autophagy. *Diabetes*. 2014;63(6):2063–2072.
29. Zhang MZ, Yao B, Fang X, Wang S, Smith JP, Harris RC. Intrarenal dopaminergic system regulates renin expression. *Hypertension*. 2009;53(3):564–570.
30. Yao B, Harris RC, Zhang MZ. Intrarenal dopamine attenuates deoxycorticosterone acetate/high salt-induced blood pressure elevation in part through activation of a medullary cyclooxygenase 2 pathway. *Hypertension*. 2009;54(5):1077–1083.